

Improvement of the EFFECTS Dispersion Model for Jets in Cross Flow

Andreas Mack

Gexcon Netherlands BV, Princenhof Park 18, Driebergen, 3972 NG, The Netherlands
andreas.mack@gexcon.com

The present paper describes the modelling of vertical jets in crossflow in the consequence modelling software EFFECTS v12.4, based on an integral modelling approach, including validation in a wide range of density variation of the released substance.

1. Introduction

Hydrogen from renewable energy sources, ammonia as an energy carrier, LNG as intermediate energy carrier solution and carbon dioxide for Carbon Capture, Utilisation and Storage (CCUS) solutions will play a major role in the energy transition. These substances exhibit substantially different specific weights, leading to different dispersion behaviors particularly if released as vertical jets in the cross flow of an atmospheric boundary layer. Modelling of vertical jets, perpendicular to the wind direction is much more challenging compared to a jets release in flow direction. Additional physical effects take place depending on the release and wind conditions. Experimental data sets in the relevant turbulence regime are scarce, particularly for lighter than air substances. This might also be due to the fact that measurement is much more complex since concentration measurements have to be performed in a 3d field with a trajectory strongly depending on buoyancy of the released substance.

2. Modelling of vertical jets in cross flow

Modelling of vertical jets, perpendicular to the wind direction of the atmospheric boundary layer (cross flow) in EFFECTS, for heavy gas releases was based on an empirical modelling approach of Ermak (1990) which has been recently improved (Mack, 2024). For releases lighter than ambient density an alternative modelling approach has been developed based on a combination of an analytical solution of a jet in cross flow for the momentum dominated region close to the release, and an integral dispersion model Mack (2024).

2.1 Modelling of vertical heavy gas releases in cross flow

As mentioned, for releases of substances with densities larger than ambient, including multiphase releases, the approach of Ermak (1990) has been applied including some modifications. The empirical model is based on data for the trajectory and concentration distributions based on experiments. The experimental data set was enlarged by measurements from Schatzmann et al. (1999), Donat (1996), Donat and Schatzmann (1999), Vidali et al. (2019) and Jack Rabbit of Gavelli et al. (2023). The trajectory and concentration modelling follows an analytical approach until the apogee of the trajectory, from there the empirical dispersion model is applied including possibly descending trajectories. The coordinates and concentration in the apogee are given in Ermak (1990). However, for low wind speeds and release terms resulting in large plume rise heights, the ambient velocity at release height taken by the original model is not valid anymore. Therefore, the ambient wind speed is corrected for an additional height, which is a fraction of the momentum dominated length. This puts a limit on the maximum plume rise height by applying a higher representative wind speed. This additional height is calculated iteratively as:

$$l_m = \sqrt{M_s}/U_a \quad (1)$$

With the ambient wind speed $U_a = U_a(h_s + l_m)$ and M_s being the source momentum flux. The Froude number

$$F_r^2 = W_s^2 / (g \cdot D_s \cdot (\rho_s - \rho_a) / \rho_a) \quad (2)$$

used in the calculation of the apogee trajectory coordinates is limited in order to improve the agreement with experimental data

$$F_{rl}^2 = F_{rmin}^2 + C_F \cdot (F_r^2 - F_{rmin}^2) \quad (3)$$

with $C_F = 0.4$ and $F_{rmin}^2 = 10$ and a maximum of 70.1 applied on the Froude number. The release velocity is W_s , ρ_s and ρ_a are the density of the source and the ambient air, D_s is the release diameter and g the gravitational acceleration.

The maximum plume rise height for non-buoyant releases h_{prm} in Ermak (1990), originally based on Brigg's plume rise equation and showing some overestimation of the plume rise height, is extended by a formulation of Chen and Rodi (1980)

$$h_{prm} = \min(3.7 \cdot \sqrt{F_r} \cdot \frac{D_s}{2}, h_{prm}) \quad (4)$$

with the source width D_s . The plume rise heights are transitioned between the non-buoyant and buoyant regime based on a blending factor of $1 - 1/(\max(1, F_r))$.

The downwind location at maximum plume rise x_{prh} is calculated by the original model and blended with a correlation of Pratte and Baines (1967) for non-buoyant releases comparable to the maximum plume rise height:

$$x_{prm} = \left(\frac{h_{pr}}{1.63}\right)^3 \frac{1}{\left(\frac{W_s}{U_a} D_s\right)^2} \quad (5)$$

The volumetric concentration at the maximum plume rise height is given by Ermak (1990) as:

$$c_{pk} = 0.845 \cdot R_v \cdot (D_s/h_{pr})^{1.85} \quad (6)$$

Here, the coefficient 0.845 was modified from 1.9 in the original publication due to better agreement with the experimental data mentioned above. The calculation of the plume speed and dimensions is based on the conservation of momentum and follows the original approach in Ermak (1990). With the ascending, empirical trajectory part the trajectory location follows an elliptical path whereas the plume variables are interpolated between the release and apogee point.

Beyond the point of maximum plume rise, the Dispersion Model is applied to calculate further dilution of the plume applying the condition at maximum plume rise as initial condition.

2.2 Modelling of light gas releases in cross flow

Light gas vertical releases in crossflow in EFFECTS are modelled in a different way compared to the release for heavy gas. Light gas vertical releases in cross flow usually reach the final plume rise at larger distances and heights from the release, therefore applying an empirical model should be restricted to the vicinity of the release in order to avoid inaccuracies in the calculation of the plume parameters which are based on interpolation in the ascending trajectory part for the heavy gas release model. Here, only the initial, usually momentum dominated region of a vertical jet in crossflow is calculated and serves as initial condition for the Dispersion Model. Therefore, the main part of the light gas vertical release dispersion is modelled directly within the Dispersion Model.

Based on similarity theory, a characteristic length scale l_m of a jet in crossflow where the momentum or buoyancy rather than the crossflow effects are dominant is given by Rodi (1982) as:

$$l_m = \sqrt{M_s} / U_a(h_s) \quad (7)$$

For a buoyant source in crossflow, a characteristic length scale based on the buoyancy flux B can be derived

$$l_b = B / U_a(h_s)^3 \quad (8)$$

With the buoyancy flux defined as $B = g \cdot (\rho_a - \rho_s) / \rho_s \cdot \dot{m}_s / \rho_s$ and the mass flow rate \dot{m}_s . The initial trajectories follow either the buoyancy ($l_m < l_b$) or momentum ($l_m > l_b$) dominated regime with the corresponding analytical solutions for the velocity components, trajectory position and dilution as given by Rodi (1982). For the modelling of the vertical light gas jet, the trajectory point at which the solution is switched from the empirical model to the Dispersion Model is not critical. Choosing the point at the momentum- or buoyancy dominated region results in

an initial stage with the model based on similarity theory. This also ensures a consistent inlet condition for the further integral modelling within the Dispersion Model.

For the momentum dominated flow the height at the trajectory point is calculated by $h_{pr} = l_m$. For the buoyancy dominated flow the height at the trajectory point is calculated by:

$$h_{pr} = \frac{M_s^{3/4}}{\sqrt{B}} \quad (9)$$

The absolute vertical coordinate of this point is then $z_{pr} = h_s + h_{pr}$. For the calculation of the corresponding downwind location the trajectory follows the similarity rule for the trajectory of momentum-based releases, since here the differences for buoyancy and momentum-based trajectories are small in the initial stage of the trajectory and for the cases considered. The downwind location is calculated by (Rodi, 1982) as:

$$x_{pr} = \frac{1}{C_1^2} \frac{h_{pr}^2}{l_m} \quad (10)$$

with the constant $C_1 = 2.5$. The mass fraction $c_{mpk}(z_{pr})$ at the trajectory point (x_{pr}, z_{pr}) centre line is also given by Rodi (1982) for a vertical release in crosswind as:

$$c_{mpk}(z_{pr}) = \frac{U_a(h_s)}{C_2 W_s} \frac{l_m}{h_{pr}} \quad (11)$$

with the constant $C_2 = 0.21$. Because both momentum- and buoyancy dominated regions use the same calculation method, this approach might be slightly conservative for buoyancy dominated flows. Investigations showed that the effects on the further dispersion process are minor.

The plume center line horizontal velocity is based on the conservation of momentum comparable to the heavy gas model explained before and follows the original approach in Ermak (1990). The centerline velocity is calculated by the model of a turbulent jet by Mack and Boot (2023), since in the momentum dominated region of the trajectory the ratio of crosswind and jet velocity is low. The vertical component is then derived from the centerline velocity $u_c(h_{pr})$ and plume horizontal velocity. The velocity components could also be derived from the analytical trajectory function which turned out to be less consistent than the chosen approach.

By using Eq(11), a full set of initial conditions are provided as input in the Dispersion Model. The conditions of the first trajectory part are interpolated between the release point and trajectory point (x_{pr}, z_{pr}) applying similarity rules comparable to the heavy gas vertical jet.

The entrainment modelling for light gas vertical jets also includes the effect of entrainment enhancement due to the presence of lateral vortices from EFFECTS v12.4 onwards. Vertical jet releases in a crossflow show enhanced mixing when the vertical jet is bent over due to the presence of the atmospheric boundary layer. In first instance, close to the release, the mixing is comparable to a vertically directed turbulent free jet, since the release velocities are usually much larger than the local wind speed and shear forces in the jet dominate the mixing process. When the local flow speed is decreasing, external forces begin to play a role bending the jet in the wind direction. The plume momentum is reduced, and the jet forms an obstacle for the surrounding flow which leads to the creation of lateral vortices at the jet. Therefore, also the development of these main lateral vortices is taken into account in the dispersion modelling for vertical jet releases. As found in comparisons with experimental data in the past and used by different models, vortices enhance the mixing process proportionally to the wind component which is perpendicular to the trajectory axis, see also Ooms (1972). These models use an additional cross flow entrainment term which is proportional to the ambient wind speed component perpendicular to the local trajectory. The additional entrainment term in EFFECTS is:

$$V_{j, cross} = C_{cross} \cdot \rho_a / \rho \cdot U_a \cdot |\sin(\vartheta)| \quad (12)$$

with ϑ being the angle between the horizontal (downwind direction) and the local trajectory tangent. C_{cross} is an entrainment constant (0.35). Literature values range from 0.4 to 0.6, where sometimes top-hat profiles are assumed. A value of 0.35 applied for gaussian profiles corresponds approximately to a value of 0.6 if top hat profiles are assumed. Comparing with experimental data, a value of $C_{cross} = 0.35$ shows good agreement between simulations and experimental data. The additional entrainment is not applied for descending trajectories of negatively buoyant plumes since lateral vortices will not develop as fast as in the strongly curved, high velocity jet region of vertical jets in crossflow. The velocity difference between plume and ambient flow is very low for descending plumes. This would lead to too high entrainment compared to experimental data.

It should be mentioned that for releases at the ground, also horseshoe vortices can be formed at the ground. Depending on the release substance and the conditions, also complex vortex systems in the wake of the release might form which cannot be modelled in detail by integral models; these effects are taken into account implicitly

by the lateral entrainment in the Dispersion Model in EFFECTS. At very low Reynolds numbers, the vortex development is significantly lower. In order to achieve reliable results, the release jet Reynolds number shall be sufficiently high (>3000) and the cross flow in the fully turbulent regime. In laminar flow conditions, concentration results might be underpredicted. Since these conditions (low turbulent or laminar) are not typical for safety related releases in atmospheric boundary layers, this regime is excluded from the validation. Therefore, experimental results obtained in the laminar regime are also invalid for the scenarios considered here and have been excluded from the validation campaign.

3. Validation results for vertical jet releases in cross flow

For vertical jet releases in crossflow, the comparison of simulations with experimental data is challenging due to the different physical phenomena being dominant during the experiments. Many experimental datasets available are focussing mainly on trajectories and velocity distributions. Data including concentration measurements are often not representative for accidentally jets released into atmospheric boundary layer, because either jet or cross flow Reynolds numbers are too low (laminar flow). This can lead to different jet behaviour with different mixing or trajectories due to low turbulence or the absence of lateral vortices in the vertical jet region. Therefore, only validation cases with representative release conditions and wind fields have been selected for validation purpose. The cases were selected including a range of light gas, non-buoyant and heavy gas releases.

Vertical jet trajectories are compared with experimental data from Pratte and Baines (1967) for different velocity ratios of jet to wind speed, ranging from 5 to 35. The simulations have been performed with a release diameter of 0.01m, resulting in a release velocity of 7.44m/s. The corresponding wind speeds are 1.49, 0.50, 0.30 and 0.21m/s. The trajectory curves are all higher than 20 times the release diameter, which minimizes local effects at the release and ensures the development of the lateral vortices. The comparison of the EFFECTS simulations show good agreement with the experimental data, as shown in Figure 1, left.

A typical lighter than air vertical release in an atmospheric boundary layer was experimentally investigated by Ooms in the KSLA wind tunnel test facility Ooms (1972). The experiment was scaled by a factor of 100 in the simulations; the release conditions for the scaled experiment are a release diameter of 0.081m, ambient wind speed 20 m/s, release velocity 170.4 m/s and a release density of 0.6 kg/s. A comparison of the simulation data of EFFECTS with the data from the experiments shows good agreement of the trajectory of the jet (Figure 1, right).

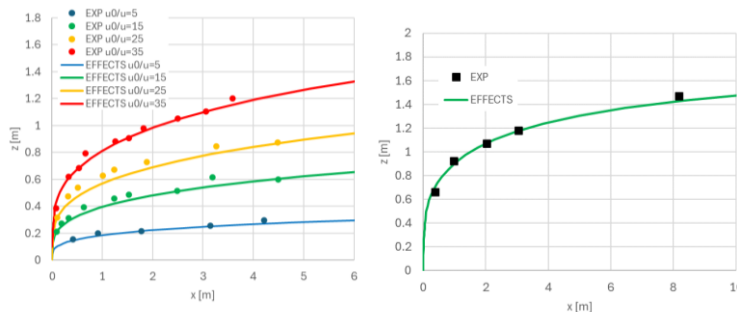


Figure 1: Comparison of experimental trajectory data and EFFECTS simulations for Pratte & Baines (1967) test case (left) and Ooms (1972) test case (right)

Extensive testing of natural gas vertical jets was performed by Birch et al. (1989) including detailed trajectory and concentration measurements. The simulations were performed with a natural gas mixture consisting of 94% methane. The release diameter is 0.01026m, release velocity 75m/s into a 5m/s wind field. The release height was 0.298m. The experimental data reports the maximum concentration in the symmetry plane and the maximum concentration in the crosswise plane. Due to the presence of the lateral vortices with the vertical jet, concentration contours in a crosswise plane are not point symmetric around the trajectory axis but elongated in lateral direction with local concentration maxima at the two lateral vortices. Due to the modelling in EFFECTS, which is an integral model approach, the concentration contours usually follow gaussian distributions such that the local maxima observed at off-centerline positions as in the experiments cannot be predicted. Therefore, the simulations always show maximum concentrations in the symmetry plane whereas the maximum is usually lower than the measured ones. The difference between the maximum concentration data at the vortex location and symmetry plane is rather low and shows an absolute difference lower than 1% for concentration levels lower than 10%. The experiments were scaled by a factor of 10 for the simulations, in Figure 2 (left) the trajectory data of the experimental data is given for the symmetry plane and the vortex location. As can be seen clearly, the

trajectory simulation corresponds better with the vortex location than with the data in the symmetry plane. This is in agreement with the expected behaviour of the integral modelling approach. In Figure 2 (right) a comparison of the concentration distributions is given, which show a slight under prediction for concentration higher than LFL (5%) but the global trend is in good agreement. Overall, the integral modelling approach used here shows minor deviations with respect to the location of the plume maximum concentration since not the full vortex system is modelled which should be taken into account, particularly when used for ignition simulations at height.

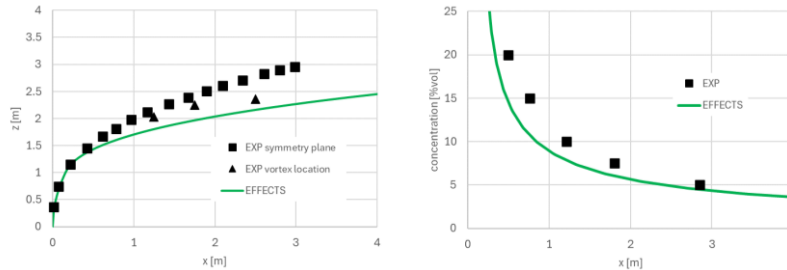


Figure 2: Comparison of experimental trajectory (left) and maximum concentration data (right) and simulations for Birch et al. (1989) experimental data

Kamotani (1971) performed experiments for turbulent jets in cross flow for heated (buoyant) and unheated jets (non-buoyant). The release diameter is 6.35mm; all velocities are based on effective velocity ratios defined as $R = \sqrt{\rho_s U_s^2 / \rho_a U_a^2}$ with ρ_s and ρ_a being the densities of source and cross flow and U_s and U_a being the velocities, respectively. Experiments are performed at source temperatures of 75°F (24°C and 320°F (160°C) above ambient temperature. For the unheated cases, the trajectory is defined by the location of the maximum velocity. For heated cases, the location of the maximum temperature defines a second, temperature based trajectory. The trajectory of the heated jet is lower (compare Figure 3, left) due to different mixing of momentum and energy in the lateral vortices. At constant R, the trajectories are more or less identical for increasing release temperatures. For the heated cases, the local temperature data can be converted to corresponding concentration data by $c = (T - T_a) / (T_s - T_a)$ with T_s and T_a being the temperature of the source and the cross flow, respectively. The simulations have been performed at a scale of 5:1.

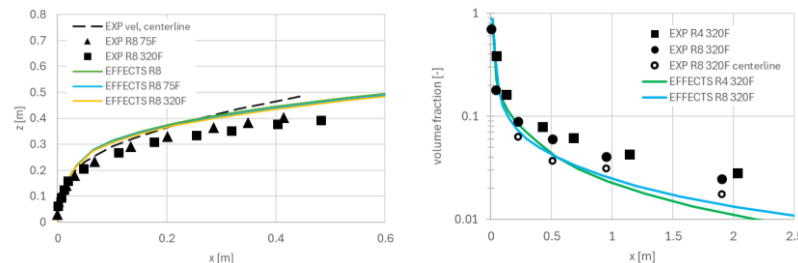


Figure 3: Kamotani (1971) experimental data and simulation results for trajectory data (left) and concentration data (right)

For $R=8$, the agreement between the experimental data and the simulation is fair for the trajectory location compared with the velocity centerline (R8, unheated) and only a slightly higher trajectory predicted for the heated cases (Figure 3, left). The trend that the increasing temperature, at constant R, does not affect the trajectory location, is well reproduced by the simulation. For $R=4$, an over prediction of the trajectory by approximately 2 release diameters is present which can still be considered minor (not shown here). The concentration distributions for $R=4$ and $R=8$ at 320°F are compared in Figure 3 (right). For $R=8$, the concentration distribution based on the maximum values (away from the symmetry plane) are slightly under predicted by the simulations for larger distances. In addition, the maximum concentrations on the centre line (symmetry plane) are given in the experiment, which are 30 to 50% lower. These values agree reasonably with simulation data of EFFECTS with a slight under prediction at larger downwind positions (Figure 3 (right)).

Extensive heavy gas release experiments were performed by Schatzmann et al. (1993). Here, only comparison results of test T10 (scale 100:1; release diameter 1.27m, release height 8.5m, mass flow rate 58kg/s, molecular weight 66.6g/mole, wind speed 6.7m/s at 10m height) is given. The simulations well reproduce the trajectory rise, the maximum height and the descending trajectory due to the negatively buoyant plume (Figure 4, left).

Also, the concentration results at the trajectory location (Figure 4, middle) and at a constant height of 1m (Figure 4, right) are in good agreement with the experimental data with a minor over prediction in the descending and far field plume area.

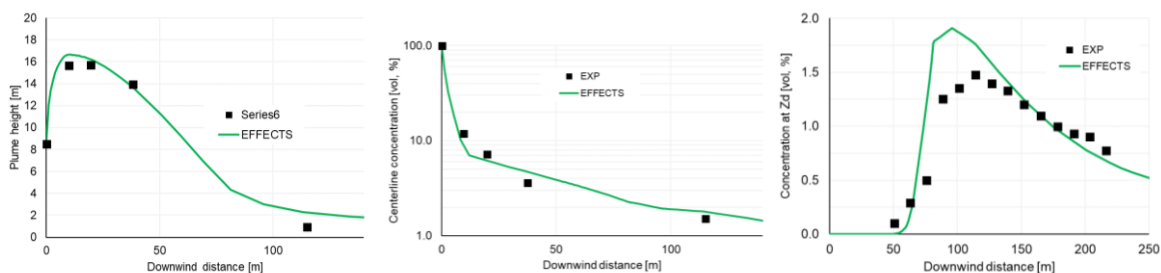


Figure 4: Schatzmann T10 experimental data and simulation results for trajectory data (left), maximum concentration (middle) and concentration at $z=1\text{m}$ (right)

4. Conclusions

The present paper describes the modelling and validation of jets in cross flow as implemented in the EFFECTS v12.4 Dispersion Model. The modelling of jets in cross flow for a wide range of release conditions from light to heavy gas releases show a reasonable agreement with the experimental data, although the flow phenomena in vertical jets are relatively complex compared to horizontal jets. The trajectory position as well as concentration distributions of the simulations reproduce the experimental data well; minor deviations from the experiments such as off-centerline maximum concentration distributions can be explained with additional 3D effects being present in the experiments. Overall, as worst case, the concentration results show a maximum deviation of 30-50%; the position of the maximum concentration location (trajectory) showed maximum 25% deviation. This should be taken into account as safety factor, particularly when estimating ignition probabilities.

References

- Birch, A. D., Brown, D. R., Fairweather, M., Hargrave, G. K., 1989, An Experimental Study of a Turbulent Natural Gas Jet in a Cross-Flow, *Combustion science and technology*, 66(4-6), 217-232.
- Chen, C.J., Rodi, W., 1980, *Vertical Turbulent Buoyant Jets: A Review of Experimental Data*. Oxford and New York, Pergamon Press (HMT - Science and Applications of Heat and Mass Transfer. Volume 4).
- Donat, J., 1996, *Windkanalexperimente zur Ausbreitung von Schwergasstrahlen*. Dissertation, Berichte aus dem Zentrum für Meeres- und Klimaforschung der Universität Hamburg, Reihe A: Meteorologie, 24.
- Donat, J., Schatzmann, M., 1999, Wind Tunnel Experiments of Single-Phase Heavy Gas Jets Released under various Angles into Turbulent Cross Flows. *Journal of Wind Engineering and Industrial Aerodynamics*, 83(1-3), 361-370.
- Ermak, D.L., 1990, *User's Manual for SLAB: An Atmospheric Dispersion Model for Denser-Than-Air-Releases*, UCRL-MA-105607, Lawrence Livermore National Laboratory.
- Gavelli, P., Hendrickson, B., Marsegan, C., Piekarz, J., 2020, PHMSA – Model Evaluation Protocol: Model Validation Database for Flammable Dispersion, 03903-RP-002, August 18, 2020.
- Kamotani, Y., Greber, I., 1971, Experiments on a Turbulent Jet in a Cross Flow, NASA CR-72893 FTAS/TR-71-62.
- Mack, A., Boot, H., 2023, Improvement of the EFFECTS Dispersion Model for Under Expanded Turbulent Jets. *Chemical Engineering Transactions*, 104, 25-30.
- Mack, A., 2024, *Dispersion Model in EFFECTS v12, Theoretical Background and Validation Report*, Gexcon, Utrecht, The Netherlands.
- Ooms, G., 1972, A New Method for the Calculation of the Plume Path of Gases emitted by a Stack. *Atmospheric Environment* (1967), 6(12), 899-909.
- Pratte, B. D., Baines, W. D., 1967, Profiles of the Round Turbulent Jet in a Cross Flow. *Journal of the Hydraulics Division*, 93(6), 53-64.
- Rodi, W. (Ed.), 1982, *Turbulent Buoyant Jets and Plumes: HMT: The Science & Applications of Heat and Mass Transfer, Reports, reviews & computer programs (Vol. 6)*, Elsevier.
- Schatzmann, M., Snyder, W. H., Lawson Jr, R. E., 1993, Experiments with Heavy Gas Jets in Laminar and Turbulent Cross-Flows. *Atmospheric Environment. Part A. General Topics*, 27(7), 1105-1116.
- Vidali, C., Marro, M., Gostiaux, L., et al., 2019, Dispersion of Heavy Gas and Passive Scalar Releases. Paper presented at: The 15th International Conference on Wind Engineering, September 1-6, 2019, Beijing, China.